Biomed Microdevices (2009) 11:817–826
DOI 10.1007/s10544-009-9298-4

Oxygen sensitivity and biocompatibility of an implantable paramagnetic probe for repeated measurements of tissue oxygenation

Guruguhan Meenakshisundaram · Edward Eteshola · Ramasamy P. Pandian · Anna Bratasz · Karuppaiyah Selvendiran · Stephen C. Lee · Murali C. Krishna · Harold M. Swartz · Periannan Kuppusamy

Published online: 26 March 2009

Abstract The use of oxygen-sensing water-insoluble paramagnetic probes, such as lithium octa-*n*-butoxynaphthalocyanine (LiNc-BuO), enables repeated measurements of pO_2 from the same location in tissue by electron paramagnetic resonance (EPR) spectroscopy. In order to facilitate direct *in vivo* application, and hence eventual clinical applicability, of LiNc-BuO, we encapsulated LiNc-BuO microcrystals in polydimethylsiloxane (PDMS), an oxygen-permeable and bioinert polymer, and developed an implantable chip. *In vitro* evaluation of the chip, performed under conditions of sterilization, high-energy irradiation, and exposure to cultured cells, revealed that it is biostable and biocompatible. Implantation of the chip in the gastrocnemius muscle tissue of mice showed that it is capable of repeated and real-time measurements of tissue oxygenation for an extended period. Functional evaluation using a murine tumor model established the suitability and applicability of the chip for monitoring tumor oxygenation. This study establishes PDMS-encapsulated LiNc-BuO as a promising choice of probe for clinical EPR oximetry.

Keywords EPR oximetry · Oxygen sensor · Particulate probe · Encapsulation · Polymer coating · Biocompatible EPR probe

1 Introduction

Measurement of concentrations of molecular oxygen (pO_2) in an accurate, reliable, and repeatable fashion is crucial to the understanding, diagnosis, and treatment of a number of pathophysiological conditions, including ischemic disease, reperfusion injury, oxygen toxicity, cancer, peripheral vascular disease, and wound healing (Hopf and Rollins 2007; Kulkarni et al. 2007; Kutala et al. 2007; Marso and Hiatt 2006; Vaupel et al. 2007). Of the several methods available for measuring oxygen concentration in tissues (Springett and Swartz 2007; Vikram et al. 2007), electron paramagnetic resonance (EPR) oximetry has some distinct advantages, including the ability to make minimally-invasive, real-time (*in vivo*), and repeated measurements of tissue oxygenation. In addition, EPR oximetry is unique in terms of its ability to provide absolute values of oxygen concentration without consuming oxygen (Khan, N. et al. 2007; Swartz 2004). Iterative measurements of pO_2, from a single location in tissue, are made possible by the use of water-insoluble crystalline probes, such as lithium phthalocyanine (LiPc) (Liu et al. 1993), lithium naphthalocyanine (LiNc) (Ilangovan et al. 2002a), or lithium octa-*n*-butoxynaphthalocyanine (LiNc-BuO)

G. Meenakshisundaram · R. P. Pandian · A. Bratasz · K. Selvendiran · P. Kuppusamy (✉)
Department of Internal Medicine, Ohio State University,
420 West 12th Avenue, Room 114,
Columbus, OH 43210, USA
e-mail: kuppusamy.1@osu.edu

E. Eteshola · S. C. Lee
Department of Biomedical Engineering, Ohio State University,
Columbus, OH 43210, USA

G. Meenakshisundaram · E. Eteshola · R. P. Pandian · A. Bratasz · K. Selvendiran · S. C. Lee · P. Kuppusamy
Davis Heart and Lung Research Institute, Ohio State University,
Columbus, OH 43210, USA

M. C. Krishna
Biophysics Spectroscopy Section, Radiation Biology Branch,
National Cancer Institute,
Bethesda, MD 20892, USA

H. M. Swartz
EPR Center for Viable Systems, Dartmouth Medical School,
Hanover, NH 03755, USA

(Pandian et al. 2003). Of these crystalline probes, LiNc-BuO has some advantages over other probes for oximetry applications, including high EPR intensity (spin density) and oxygen sensitivity, and long-term stability and responsiveness to oxygen *in vivo* (Khan et al. 2008; Khan, M. et al. 2007; Mohan et al. 2009; Wisel et al. 2007). Although, LiNc-BuO can be used in its neat crystalline form to measure oxygen, its direct *in vivo* application may be limited by particle migration within tissue leading to loss of EPR signal intensity over time, and potential biocompatibility concerns due to direct exposure of crystals to tissue.

Encapsulation or coating of crystalline probes is a strategy, employed in the past, to overcome the limitations associated with these probes, and to enhance their use for clinical application (Dinguizli et al. 2006; Eteshola et al. 2009; Gallez and Mader 2000). Recently, we have encapsulated LiNc-BuO in polydimethylsiloxane (PDMS), a well-characterized, biocompatible, and highly oxygen-permeable polymer, for the development of implantable, and surgically retrievable, EPR probe formulations (denoted as LiNc-BuO:PDMS chips) (Meenakshisundaram et al. 2009). Fabrication, by cast-molding/polymerization methods, and physical characterization of LiNc-BuO:PDMS chips demonstrated that encapsulation in the PDMS matrix did not have any significant effect on the oxygen-sensing ability of the embedded LiNc-BuO microcrystals. The cast-molding procedure also facilitated the fabrication of chips with different sizes, shapes and spin densities (Meenakshisundaram et al. 2009). In the present study, we report the biological evaluation and functional testing of LiNc-BuO:PDMS chips, including *in vitro*/*in vivo* biocompatibility and oxygen-sensing performance. The study demonstrated that the encapsulation of LiNc-BuO microcrystals in PDMS does not interfere with their oxygen-sensing ability, while enhancing their biocompatibility and suitability for direct *in vivo* application.

2 Materials and methods

2.1 Fabrication of LiNc-BuO:PDMS chips

LiNc-BuO was synthesized as microcrystalline powder as reported (Pandian et al. 2003). Different batches (preparations) of LiNc-BuO are known to exhibit slight variations in their oxygen sensitivities (Pandian et al. 2006), and hence we have tried to use a single batch of LiNc-BuO for most of the experiments in this study. Polydimethyl siloxane (PDMS) was obtained as medical grade Silastic (MDX4-4210) from Dow Corning (Midland, MI). LiNc-BuO:PDMS chips were fabricated by cast-molding and polymerization as reported (Meenakshisundaram et al. 2009).

2.2 Oxygen calibration and spin density evaluation

Calibration of the oxygen response and evaluation of spin density of the LiNc-BuO:PDMS chip were done, using an X-band EPR spectrometer, as reported (Meenakshisundaram et al. 2009). Calibration of the LiNc-BuO:PDMS chip that was explanted from the muscle tissue was performed using an L-band EPR spectrometer (Pandian et al. 2003).

2.3 Autoclaving and UV-sterilization

Autoclaving was performed using a bench-top analog sterilizer (Tuttnauer® by Brinkmann Instruments, New York) at the following settings: 121°C for 1 hour at 1 atm. pressure (wet cycle using steam), followed by exhaust-drying for 15–20 min. UV-sterilization was carried out by exposing the chips to UV light, for 1 hour, in a laboratory cell-culture hood.

2.4 High-energy irradiation

^{60}Co γ-radiation (30 Gy dose) was performed using an Eldorado 8 Cobalt-60 Teletherapy machine (Theratronics International, Ontario, Canada). Chips were irradiated with X-rays using a linear accelerator (Siemens Medical Solutions, Malvern, PA). A dose of 30 Gy, with 6 MeV at a rate of 3 Gy/min, was delivered. The choice of radiation dose was based on clinical relevance.

2.5 Oxidoreductant treatment

The effect of the following oxidants and reductants, on the oxygen calibration and spin density of the LiNc-BuO:PDMS chip, were evaluated: superoxide, nitric oxide, hydrogen peroxide, glutathione, and ascorbate. Superoxide was generated by adding 0.02 U/ml of xanthine oxidase to a 0.2-mM xanthine solution. Nitric oxide was produced using a 5-mM solution of S-nitroso-N-acetyl penicillamine (SNAP) in distilled water. Hydrogen peroxide was used at a final concentration of 1 mM. Ascorbate (1 mM) and glutathione (5 mM) were prepared in distilled water. All chemicals were obtained from Sigma-Aldrich (St. Louis, MO), except SNAP which was obtained from Invitrogen (Eugene, OR). LiNc-BuO:PDMS chips were exposed by immersing in solutions of the oxidoreductants for 30 min, followed by drying (in air) for 60 min, before EPR measurements were made.

2.6 Assessment of *in vitro* biocompatibility

Chinese hamster ovary cells (CHO), cisplatin-sensitive human ovarian cancer cells (A2780), cisplatin-resistant

human ovarian cancer cells (A2780 cDDP), and smooth muscle cells (SMC) were seeded into 96-well microplates at a density of $1x10^4$ cells/well, in complete RPMI-1640 medium (200 µl/well). SMCs were cultured using the same protocol, except using complete SMC basal medium. The seeded cells were cultured for 24 h at 5% CO_2, 37°C, and 95% humidity, before autoclaved LiNc-BuO:PDMS chips were added to the culture medium. The cells were allowed to incubate with the chips for 48 h, after which cell viability and proliferation were evaluated. Assessment of cell viability was performed using the colorimetric MTT assay (Denizot & Lang 1986). Cell proliferation was determined using the anti-BrdU immunoassay (Cell Proliferation ELISA, BrdU, Roche Diagnostics, Germany). Data obtained (n=6), in the form of optical density, were expressed as a percentage relative to control.

2.7 Animal procurement and handling

Female C3H mice, used in this study, were obtained from Frederick Cancer Research Center, Animal Production Unit (Frederick, MD, USA). The animals were received at 6 weeks of age and housed five per cage in climate- and light-controlled rooms. Food and acidified water were allowed *ad libitum*. At the time of experiment, animals were 50-days old and weighed approximately 25 g. Animals were used according to the Public Health Services Policy, the Federal Welfare Act, and the Ohio State University Institutional Laboratory Animal Care and Use Committee (ILACUC) procedures and guidelines.

2.8 RIF-1 tumor growth

Culture of RIF-1 cells and subsequent injection of cells in the hind leg of mice were performed as described (Bratasz et al. 2007). The size of the tumor was monitored daily, after injection of cells in the hind limb, using digital Vernier calipers. Tumor volume was calculated using the formula $(d_1 \text{ X } d_2 \text{ X } d_3)\pi/6$, where d_1, d_2, and d_3 represent the orthogonal dimensions of the tumor. The tumor was allowed to grow for a week (volume of approximately 1 cm^3), before LiNc-BuO:PDMS chips were implanted.

2.9 Anesthesia

For the implantation of LiNc-BuO:PDMS chips in muscle and tumor, as well as, long-term oxygen measurements in muscle tissue, animals were anesthetized by intraperitoneal administration of ketamine and xylazine (200 mg/kg body-weight and 4 mg/kg body weight, respectively). Tumor oxygenation was measured under isoflurane anesthesia (1.5%, mixed with room air as the breathing gas). The mixture was delivered to the animals using a veterinary anesthesia system, Vasco Anesthesia (Pro Tech Medical, Illinois). The flow rate of room air was maintained at 1.5 liter/min. The animals were secured to a plastic bed plate fitted with a custom-made nose cone, through which the breathing gas and anesthesia were delivered. Excess breathing gas in the delivery system was suitably ventilated to maintain the pressure in the system. MR imaging, for identifying the location of the implanted chips in the tumors, was also performed under isoflurane anesthesia.

2.10 Implantation of LiNc-BuO:PDMS chips in tissue

LiNc-BuO:PDMS chips were implanted subcutaneously in the gastrocnemius muscle of the right hind limb of the animals. A small flap of skin was cut and a LiNc-BuO:PDMS chip (~2 mm×2 mm) was inserted into the muscle tissue, before the flap was sutured back in place. The sutured skin was allowed to heal for at least 24 h prior to making EPR measurements. For implantation in RIF-1 tumors, LiNc-BuO:PDMS chips (approximately 3 mm× 1 mm) were loaded into 21-gauge needles, which were then inserted into the tumors. A thin wire stylus, which fit into the bore of the needle, was used to push the chips into the tissue. In each animal, a LiNc-BuO:PDMS chip (3 mm× 1 mm) was also implanted in the gastrocnemius muscle of the hind limb contralateral to the tumor (internal control).

2.11 Magnetic resonance imaging (MRI)

MRI was performed to confirm the location of the implanted LiNc-BuO:PDMS chip in the tumor tissue. Images were acquired using an 11.7 T system (Bruker Biospin, Billerica, MA), employing a Rapid Acquisition with Refocused Echo (RARE) protocol. Image acquisition parameters were as follows: repetition time (TR)=6000 ms, echo time (TE)=34 ms, slice thickness=1 mm, field of view=28 x 28 mm, matrix size=256 x 256 pixels, RARE factor=8.

2.12 *In vivo* EPR measurements

Measurements of muscle and tumor oxygenation were performed using an L-band (1.2 GHz) spectrometer (Magnettech, Berlin, Germany) using a surface-loop resonator. Animals were placed on a plastic bed plate such that the location of chip-implantation in the muscle or tumor was just beneath the loop, and approximately centered at the active surface of the loop resonator. Body temperature, during measurements, was monitored using a thermistor rectal probe, and maintained at 37±1°C using an infrared lamp.

Post-implantation pO_2 measurements in muscle were made every week, for up to 70 days. In order to verify that

the implanted LiNc-BuO:PDMS chip was sensitive to changes in tissue oxygenation, the muscle tissue was subjected to constriction of blood flow, thereby a reduction in oxygen supply, to the hind limb. This was achieved by gently tying the limb above the location of chip implantation using an elastic band. The constriction was maintained in place until EPR measurements were made (usually less than 5 min) and then removed. One animal was subjected to constriction every week, and each animal was constricted three times, on different days, during the course of the experiment. In order to verify that the LiNc-BuO:PDMS chip implanted in RIF-1 tumors was responsive to changes in tumor pO_2, the animals were subjected to an oxygen challenge, *viz.* carbogen-breathing. EPR spectral acquisition was carried out continuously throughout the course of the carbogen-breathing challenge, which was designed as follows: baseline measurements of pO_2 were made under room air-breathing (40 min), which was followed by carbogen-breathing for 45 min. Subsequently, the breathing gas was switched back to room air, and EPR measurements were continued for another 30–45 min.

2.13 Histology

At the end of the long-term pO_2 measurements in muscle, animals were sacrificed and muscle tissues, with implanted LiNc-BuO:PDMS chips were excised. Tissues, with embedded chips, were fixed in paraformaldehyde, and then sectioned in paraffin (slice thickness: 4 μm). Tissue slices were mounted on glass slides and stained with hematoxylin and eosin stain (H&E). Images of the slides were acquired using an inverted light microscope (Nikon TE2000-U, Nikon, Melville, NY) and analyzed using MetaMorph software (Molecular Devices, Downingtown, PA).

2.14 Statistical analysis

Data were expressed as mean ±SD and compared using a Student's t-test with the level of significance (p) set at 0.05.

3 Results and discussion

3.1 Effect of sterilization

Any biomaterial intended for implantation and *in vivo* application needs to be sterilized, in order to minimize the adverse effects of infection and subsequent rejection of the implanted material. As a result, evaluation of the effects of sterilization on the intended functionality of the implant, the LiNc-BuO:PDMS chip in this case, is of paramount importance to ensure safety and efficacy of *in vivo* performance. We studied the effect of autoclaving and UV-treatment on the oximetry properties of the LiNc-BuO:PDMS chip. Figure 1 ((a) and (b)) show the effect of these two sterilization procedures on the oxygen calibration and spin density of the LiNc-BuO:PDMS chip, respectively. The results showed that the oxygen calibration of the chip was unaffected by sterilization. The calibration curves were linear before and after treatment, while the oxygen sensitivity (slope of the curve) after autoclaving, and UV-treatment were not significantly different from control. Also, spin density of the LiNc-BuO:PDMS chip was not affected by either sterilization procedure, compared to unsterilized control.

The sterilization results demonstrated the durability of the LiNc-BuO:PDMS chips, given that autoclaving is a very rigorous sterilization method involving high temperature and pressure conditions. The high temperature (121°C) could lead to degradation of the polymer matrix, leading to loss of oxygen permeability of the polymer. Such degradation may cause the deformed polymer to block the channels and prevent free diffusion of oxygen to the embedded crystals, affecting their oximetry property. However, the temperature range for degradation of PDMS is reported to be approximately 300–350°C (Dvornic 2000), thereby precluding any concerns with the loss of oxygen permeability due to a change in the physical properties of the polymer. In addition, the unencapsulated LiNc-BuO is reported to be stable up to 250°C (Pandian et al. 2006), which is much higher than the autoclave temperature. Therefore, the LiNc-BuO crystals would not be damaged by the treatment, keeping the molecular framework of the crystalline structure, and hence their oxygen sensitivity, intact. Similarly, UV-treatment could lead to cross-linking of polymer chains, which may have an adverse effect on oxygen permeability of the polymer. However, in this case, UV-treatment was carried out after the polymer was completely cured. Hence, any further cross-linking was not expected to occur in the PDMS matrix. In addition, it is evident from the results that the UV-treatment did not have any effect on the polymer properties, since the oxygen-sensing of the embedded LiNc-BuO remained unaffected. Further, unencapsulated LiNc-BuO is known to be resistant to high-energy irradiation (Pandian et al. 2003).

3.2 Effect of high-energy irradiation

One of the intended applications of the LiNc-BuO:PDMS chip is tumor oximetry. The level of oxygenation in the tumor tissue is a critical parameter that is considered by physicians to decide the course (dose and frequency) of chemo or radiation therapies. Treatment of the tumor with high-energy radiation will lead to exposure of the LiNc-BuO:PDMS chip to such radiation. In order to check if exposure to high-energy radiation caused any damage to the

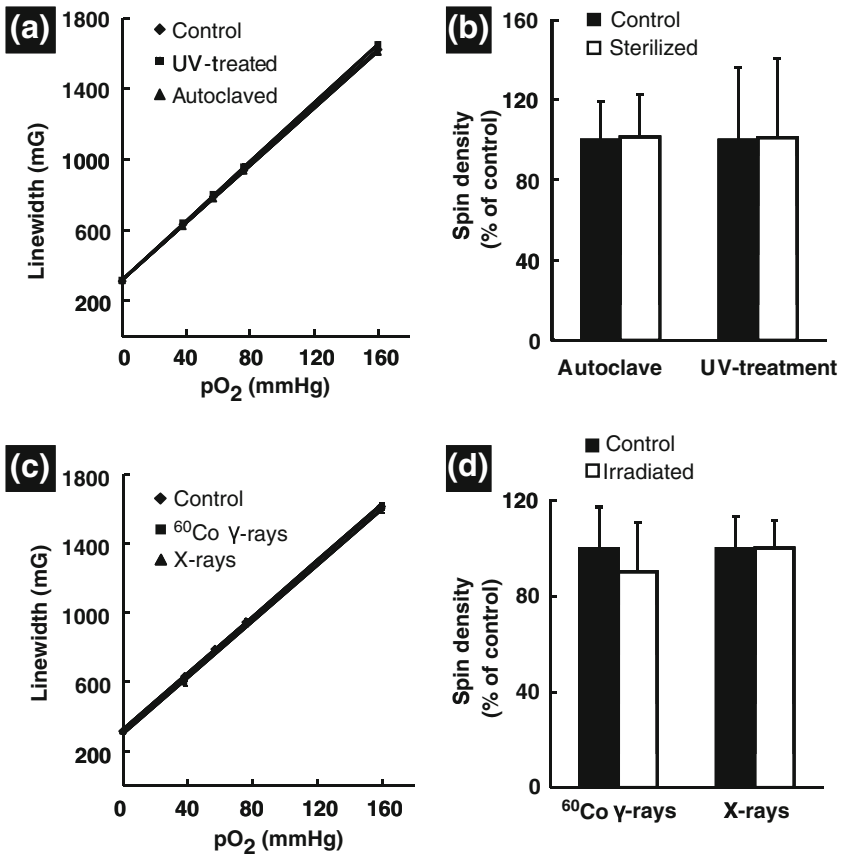

Fig. 1 Effect of sterilization and high-energy irradiation on the LiNc-BuO:PDMS chip. The effect of sterilization (autoclaving and UV-treatment) and high-energy irradiation (X-rays and ^{60}Co-γ rays) on the oxygen calibration and spin density of the LiNc-BuO:PDMS chip was evaluated using X-band EPR spectroscopy. (**a**) Effect of sterilization on the oxygen calibration of LiNc-BuO:PDMS chips (n=3). The oxygen response of the chip remained linear over the range of oxygen partial pressures (pO_2: 0–160 mmHg) used, irrespective of the mode of sterilization. The oxygen sensitivity after autoclaving and UV-treatment was 7.14±0.04 mG/mmHg and 7.35±0.11 mG/mmHg respectively. These values were not significantly different from the sensitivity of unencapsulated (neat) LiNc-BuO (7.20±0.02 mG/mmHg). (**b**) Effect of sterilization on the spin density of the LiNc-BuO:PDMS chip. Spin density was estimated using a standard of known spin density, before and after the sterilization procedures. Results (mean ± SD, n=3), normalized to respective untreated control, indicate no significant difference in estimated spin density compared to control in both cases. (**c**) Effect of high-energy irradiation on the oxygen calibration of the LiNc-BuO:PDMS chip. The oxygen response of the LiNc-BuO:PDMS chip was unaffected by exposure to 30 Gy doses of ionizing radiation, *viz.* X-rays and ^{60}Co γ-rays. Change in EPR linewidth was linear with increasing oxygen partial pressure, with no significant change in sensitivity (8.14±0.06 mG/mmHg for X-irradiation and 8.08±0.17 mG/mmHg for ^{60}Co γ-irradiation, compared to 8.12±0.01 mG/mmHg for control) (**d**) Effect of high-energy irradiation on the spin density of the LiNc-BuO:PDMS chip. Spin density (mean ±SD, n=3), calculated using a known standard and normalized to control, revealed no significant difference between irradiated LiNc-BuO:PDMS chips and control (none irradiated) chips. Results show that the functionality of the LiNc-BuO:PDMS chip was unaffected by sterilization and exposure to high-energy radiation, thereby demonstrating its stability and durability

oximetry properties of the LiNc-BuO:PDMS chip, we exposed the chips to clinically relevant doses (30 Gy) of ^{60}Co γ-rays and X-rays. The results (Fig. 1(c)) showed that the oxygen response of the LiNc-BuO:PDMS chip was unaffected by exposure to either type of radiation. The calibration remained linear with no significant difference in oxygen sensitivity before and after irradiation. In addition, the spin density of the LiNc-BuO:PDMS chip after exposure to γ- or X-rays was not significantly different from control (Fig. 1(d)).

It is noteworthy that the chips were exposed directly to 30-Gy doses of either type of radiation. However, if an equivalent dose were to be administered in a clinical situation, the amount of radiation experienced by the implanted chip will be much less due to absorption by surrounding tissue. Consequently, our rigorous experimental conditions confirmed the durability of the LiNc-BuO:PDMS chip and established its suitability for *in vivo* tumor oximetry. In addition, high-energy irradiation can also be used for sterilization of any implantable material. Given that the functionality of the LiNc-BuO:PDMS chip was not affected by exposure to high-energy radiation, such treatment could be used as an alternative to autoclaving or UV-treatment for sterilization.

3.3 Effect of biological oxidoreductants

The *in vivo* milieu is characterized by the presence of numerous oxidizing and reducing agents (oxidoreductants), and exposure to such agents may have an adverse effect on the oxygen-sensing properties of the implanted LiNc-BuO:PDMS chip. Therefore, *in vitro* evaluation of the biostability of the LiNc-BuO:PDMS chip is crucial to ensure successful *in vivo* functionality. In order to test the biostability of the LiNc-BuO:PDMS chip *in vitro*, we exposed chips to biological oxidoreductants, namely superoxide, hydrogen peroxide, nitric oxide, ascobrate and glutathione. Figure 2 ((a) and (b)) show the effect of *in vitro* oxidoreductant exposure on the oxygen calibration and spin density of the LiNc-BuO:PDMS chip, respectively. Treatment with superoxide, hydrogen peroxide, ascorbate and glutathione did not have any significant effect on the linearity and slope of the oxygen calibration. Further, treatment with any of these oxidoreductants did not have a significant effect on the spin density of the LiNc-BuO:PDMS chip.

However, treatment with nitric oxide (NO) resulted in a statistically significant decrease in oxygen sensitivity compared to control (Fig. 2(a)). NO is paramagnetic and is known to get into the channels of phthalocyanine-based crystalline EPR probes, and compete with oxygen for interaction with the probe, leading to line-broadening effects (Ilangovan et al. 2002b). However, it should be noted that NO was generated using 1-mM SNAP, which produces a large amount (several μM) of NO, while the physiological concentration of NO is in the range of 1-10 nM (Zweier et al. 1995). In contrast, the dissolved oxygen concentration in biological tissues is reported to be in the order of 1–100 μM (Zweier et al. 1995), which is at least an order of magnitude higher than the normal *in vivo* levels of NO. Therefore, in biological applications the line-broadening measured by the implanted chip would be almost entirely due to oxygen. In addition, the decreased sensitivity of LiNc-BuO:PDMS with NO treatment, although statistically different from control, was still within an acceptable range for successful application. Overall, these results suggest that the LiNc-BuO:PDMS chip can be employed successfully for *in vivo* applications, even under extreme conditions, without major concerns about the integrity of the data obtained.

3.4 *In vitro* biocompatibility

Prior to testing the *in vivo* performance of the LiNc-BuO:PDMS chip, we evaluated its *in vitro* biocompatibility by co-incubating cultured cells with autoclaved LiNc-BuO:PDMS chips for 48 h, and determining cell viability and cell proliferation using colorimetric assays. Cell viability

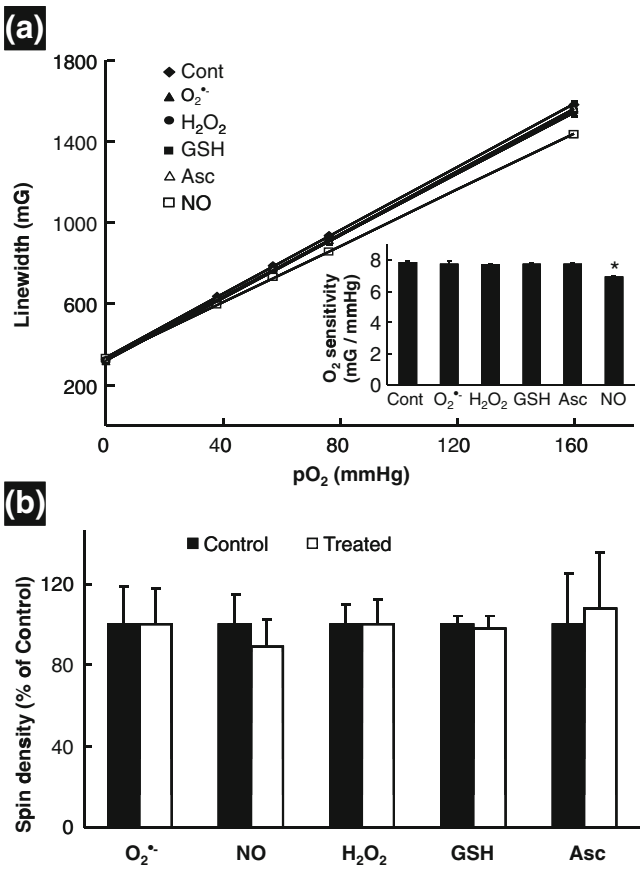

Fig. 2 Effect of oxidoreductant treatment on the LiNc-BuO:PDMS chip. (**a**) Effect of oxidoreductant treatment on the oxygen calibration of the LiNc-BuO:PDMS chip. LiNc-BuO:PDMS chips were exposed to superoxide ($O_2^{\bullet-}$) generated using 0.02 U/ml of xanthine oxidase and 0.2 mM of xanthine, nitric oxide (NO) generated using 5-mM S-nitroso-N-penicillamine (SNAP), 1-mM hydrogen peroxide (H_2O_2), 1-mM ascorbate (Asc) and 5-mM glutathione (GSH) for 30 min. After drying the samples in air, oxygen calibration of the samples was performed, using X-band EPR spectroscopy, for untreated control (Cont) and treated samples. Data are represented as mean ±SD (n=3). The calibration curves show that the response was linear with increase in oxygen partial pressure after treatment with all five agents. Inset shows oxygen sensitivities (slopes of calibration curves) of untreated control and chips treated with the oxidoreductants. Treatment with $O_2^{\bullet-}$, H_2O_2, Asc, and GSH did not significantly affect the oxygen sensitivity of the chip. A statistically significant ($p<0.05$) decrease in sensitivity, compared to control, was observed with NO treatment. However, this decrease was still within an acceptable range for potential applicability. (**b**) Effect of oxidoreductant treatment on the spin density the LiNc-BuO:PDMS chip. Active spin densities of LiNc-BuO:PDMS chips (untreated control and treated with oxidoreductants) were estimated using X-band EPR spectroscopy. Each treatment group had a separate control, and calculated spin density values were normalized to respective controls (expressed as mean ±SD, n=3). The oxidoreductant treatment did not have any significant effect on the spin density of the LiNc-BuO:PDMS chip. Overall, the results demonstrate that the LiNc-BuO:PDMS chip is biostable and unaffected by treatment with oxidoreductants

results did not reveal any significant difference between cells that were cultured without LiNc-BuO:PDMS chips in the culture media (control) and cells that were co-incubated with LiNc-BuO:PDMS chips (data not shown). In addition, exposure of the cells to LiNc-BuO:PDMS chips, by co-incubation in their culture medium, did not have any significant effect on the cell proliferation (Fig. 3). Oxygen calibration of the chips was verified after exposure to the cultured cells, with no significant difference between control chips and chips co-incubated with cells (data not shown). Results demonstrated that the LiNc-BuO:PDMS chip possessed excellent *in vitro* biocompatibility.

3.5 Long-term *in vivo* oxygen-sensing response

In order to evaluate the long-term *in vivo* oximetry capability of the LiNc-BuO:PDMS chip, we implanted the chip in the gastrocnemius muscle tissue of mice and monitored *in vivo* muscle oxygenation for up to 70 days using L-band EPR spectroscopy. Muscle pO_2 was measured every week, after implantation, for 10 weeks. Results, shown in Fig. 4(a), demonstrated the ability of the implanted LiNc-BuO:PDMS chip to provide repeated measurements of *in vivo* tissue oxygenation over the 70-day duration. Further, in order to verify if the implanted chip was responsive to changes in tissue pO_2, blood flow to the muscle was temporarily constricted using an elastic band and subsequently released. The decrease in blood flow, during the constriction, would lead to a decrease in oxygen supply to the muscle tissue. Hence, we hypothesized that the implanted chip would be able to sense the change in muscle pO_2 during constriction. Figure 4(b) shows that the implanted chip was capable of reporting the change in tissue oxygenation induced by the muscle constriction. Only one animal was subjected to constriction per week, and three such measurements were obtained from each animal during the course of the study (70 days). Such an approach, of

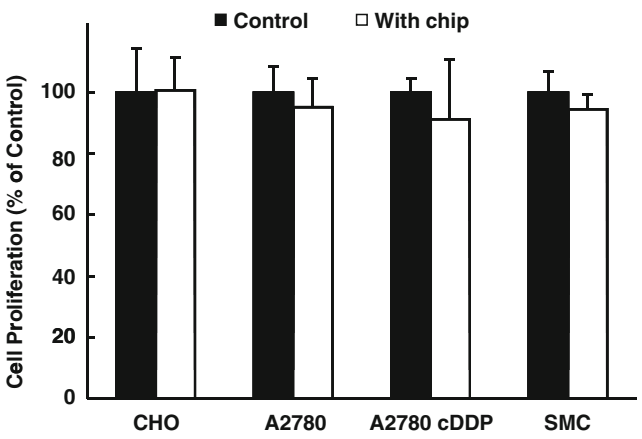

Fig. 3 *In vitro* biocompatibility of the LiNc-BuO:PDMS chip. *In vitro* biocompatibility was evaluated by assessing proliferation of cultured cells, using anti-BrdU colorimetric immunoassay. Chinese hamster ovary cells (CHO), cisplatin-sensitive human ovarian cancer cells (A2780), cisplatin-resistant human ovarian cancer cells (A2780 cDDP), and smooth muscle cells (SMC) were co-incubated with LiNc-BuO:PDMS chips, in their culture media for 48 h, after which cell proliferation was assessed. Data (mean ±SD, n=6) from cells exposed to chips, normalized to control values, showed no significant difference in cell proliferation (compared to control). Results indicate that the LiNc-BuO:PDMS chip exhibited excellent *in vitro* biocompatibility

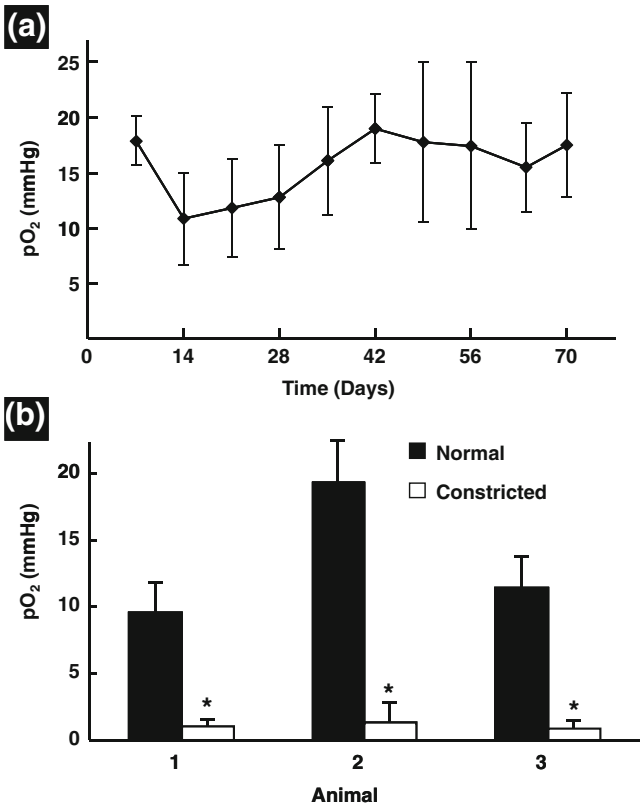

Fig. 4 Long-term *in vivo* oxygen-sensing response of the LiNc-BuO:PDMS chip. (**a**) Measurements of pO_2, from the gastrocnemius muscle tissue of mice reported by implanted LiNc-BuO:PDMS chips are shown. *In vivo* pO_2 measurements were made using L-band EPR spectroscopy for up to 70 days. pO_2 values obtained are expressed as mean ±SD (n=3). Data confirm the ability of the LiNc-BuO:PDMS chip to make repeated measurements of *in vivo* oxygenation. (**b**) Response of the LiNc-BuO:PDMS chip blood-flow constriction. Muscle pO_2 , in the constricted state, was measured from each animal on three different days during the experiment (presented as mean ±SD). Data show that the implanted chip was capable of responding to changes in pO_2. Constricted muscle pO_2 values were significantly different ($p < 0.05$) from normal muscle pO_2 values (control). Collectively, the data demonstrate that the LiNc-BuO:PDMS chip was capable of reporting oxygenation of murine muscle tissue over a period of 70 days, and possibly longer

subjecting one animal to constriction per measurement, was employed to ensure minimal trauma to the animals. The muscle pO_2 also returned back to normal levels when the constriction was removed (data not shown). Comparison of constricted-state pO_2 readouts with normal muscle pO_2, for each animal, revealed a significant difference between the two, confirming that the constriction was effective and that the chip was able to accurately sense the changes in muscle pO_2.

The implanted LiNc-BuO:PDMS chip reported an average muscle pO_2 of 15.6±2.9 mmHg, which is within the range of mouse gastrocnemius muscle pO_2 values reported previously, using unencapsulated LiNc-BuO (19.6±2.1 mmHg) (Pandian et al. 2003), LiNc (17.6± 2.5 mmHg) (Ilangovan et al. 2002a), LiPc (18±4 mmHg) (Ilangovan et al. 2004a), and TAF-coated LiPc (15.5± 1.5 mmHg) (Eteshola et al. 2009). This observation serves to validate the accuracy of the muscle pO_2 information obtained using the LiNc-BuO:PDMS chip. However, the progression of pO_2 data (Fig. 4(a)) shows an initial decrease (through day28) and a subsequent recovery in muscle pO_2. Although the mean pO_2, at each measurement point during the experiment, was still within the range of normoxic murine gastrocnemius muscle pO_2 (10–25 mmHg) (Ilangovan et al. 2004a; Ilangovan et al. 2001; Ilangovan et al. 2002a; Eteshola et al. 2009; Ilangovan et al. 2004b), there was an observable decrease in pO_2 during the initial few weeks following implantation. A similar, but unexplained, decrease in pO_2, reported by retrievable TAF micro-inserts containing LiPc, was also observed by Dinguizli et al. after 4 weeks of residence in mouse gastrocnemius muscle (Dinguizli et al. 2008). We think that such a decrease in pO_2 could be due to increased oxygen consumption by polymorphonuclear lymphocytes (PMNs), which are the first line of defense in the body's reaction to any implanted (foreign) biomaterial. It has been reported that activated PMNs increase their oxygen consumption to produce free radicals, in a phenomenon termed as 'oxidative burst', in their attempt to defend the body against any inflammatory insult (Anderson 1993). Activation of PMNs by the implantation of foreign materials and subsequent degradation of these materials has been studied previously (Labow et al. 2001). Although we do not have specific evidence to support the potential role of PMNs in modulating the oxygen response of the LiNc-BuO:PDMS chip, we speculate that the PMN oxidative burst may be responsible for the observed trend in muscle pO_2. In addition, the *in vitro* biostability of the LiNc-BuO:PDMS chip to high levels of oxidoreductants, as demonstrated in Fig. 2, suggests that the *in vivo* functionality of the implanted chip would not be affected adversely by the potentially high levels of oxygen-free radicals that may be produced by the PMNs.

3.6 Long-term *in vivo* biocompatibility and biodurability of the LiNc-BuO:PDMS chip

Any foreign material that is implanted in the body will elicit a host response. In order to assess the long-term *in vivo* biocompatibility of the LiNc-BuO:PDMS chip, we performed histological analysis of excised muscle tissue surrounding the implant. It was observed (Fig. 5(a)) that

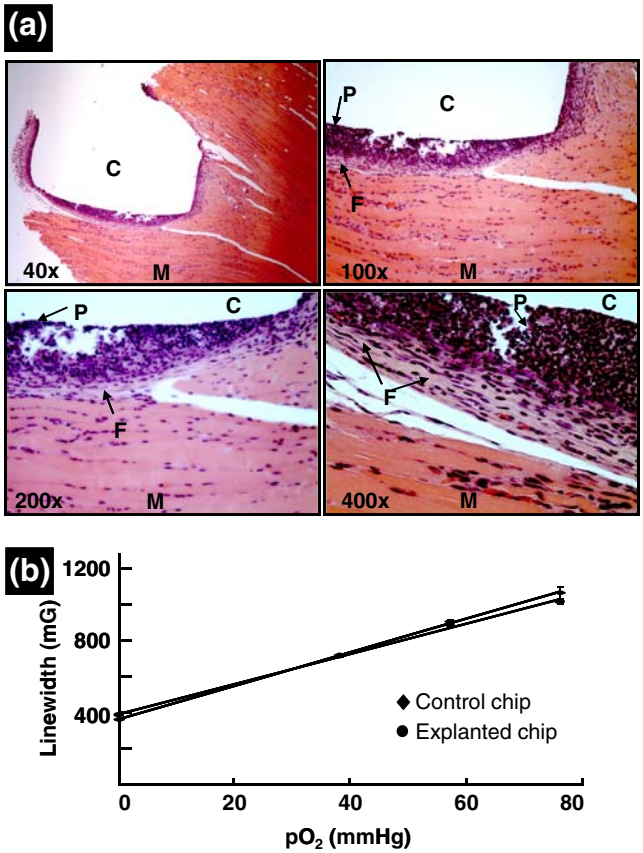

Fig. 5 *In vivo* biocompatibility of the LiNc-BuO:PDMS chip. (**a**) Images of the tissue sections, stained with hematoxylin and eosin, obtained using a light microscope at four different magnifications (40x, 100x, 200x, and 400x). The region where the implant was present is indicated as 'C' in the images, while the normal muscle tissue is depicted as 'M'. The letters 'P' and 'F' denote the dark nuclei of polymorphonuclear leukocytes (PMNs), and the pink band of fibrous tissue encapsulating the implant area, respectively. Images demonstrate that the implant triggered an acute inflammatory response, with minimal fibrous encapsulation. Average capsule thickness, estimated using MetaMorph software, was 34.89±11.05 µm. (**b**) Oxygen calibration of the LiNc-BuO:PDMS chip that was explanted from the gastrocnemius muscle tissue of mouse, after long-term implantation (70 days). Peak-to-peak linewidths at different levels of pO_2, obtained using L-band EPR spectroscopy, were used to construct the calibration curves. It can be seen that the calibration was linear for both the unimplanted control and the explanted LiNc-BuO:PDMS chip. Data (mean ±SD, n=3) show that the slopes of the two curves (oxygen sensitivity) were not significantly different (8.6±0.64 mG/mmHg for control and 9.18±0.28 mG/mmHg for the explanted chip). Results show that the LiNc-BuO:PDMS chip exhibited good *in vivo* biocompatibility and biodurability

the implanted chip elicited a characteristic wound-healing response, with the recruitment of inflammatory cells and the formation of a thin fibrous capsule. Numerous dark nuclei at the interface represent polymorphonuclear leukocytes (PMNs). The presence of PMNs demonstrates that the implant triggered an acute inflammatory response, which is normally expected of any foreign material that is implanted. The pink band of tissue (indicated by the 'F' in the images), between the inflammatory cells and the underlying muscle tissue, represents the fibrous capsule. The average thickness of the capsule was 34.89±11.05 μm, and indicated that the fibrous encapsulation was minimal. It must be noted that the acute inflammatory response and subsequent formation of a fibrous capsule did not have any significant effect on the *in vivo* oxygen-sensing ability of the LiNc-BuO:PDMS chip.

Figure 5(b) shows the oxygen calibration of the LiNc-BuO:PDMS chip that was excised from the muscle tissue after 70 days of *in vivo* residence. It was observed that the calibration remained linear, with no significant difference in oxygen sensitivity, compared to a control chip that was not implanted in the animal. The results demonstrate the biodurability of the LiNc-BuO:PDMS chip, with almost no effect on the intended functionality of the chip due to extended *in vivo* residence.

3.7 Tumor oximetry using the LiNc-BuO:PDMS chip

Having established the suitability of the LiNc-BuO:PDMS chip for *in vivo* oximetry, we evaluated its applicability for providing therapeutically-useful pO_2 information in a clinically relevant animal model of disease. We chose a murine RIF-1 tumor model for testing the functional performance of the chip.

Figure 6(a) shows a representative MR image of the RIF-1 tumor implanted with the LiNc-BuO:PDMS chip. The purpose of the MR imaging was to verify that the chips were not implanted in the core of the tumor, which is usually characterized by poor blood perfusion, necrotic cells, and hypoxic pO_2 (Bratasz et al. 2007). The location of the chip within the tumor was important to determine, because if located in the anoxic core of the tumor, the chip may be predisposed to reporting a near-anoxic pO_2 value, and not responding to real-time changes in tumor oxygenation. However, care was taken during the implantation procedure to adjust the depth of needle insertion, and make sure that the chips were not implanted in the core of the tumor. This is evident from the MR image.

Tumor pO_2 measurements were made on the second day after implantation of chips. Figure 6(b) shows pO_2 values measured from tumor and muscle (internal control). Data show that the chip was able to sense the hypoxia in the tumors, with a significant difference in pO_2 compared to

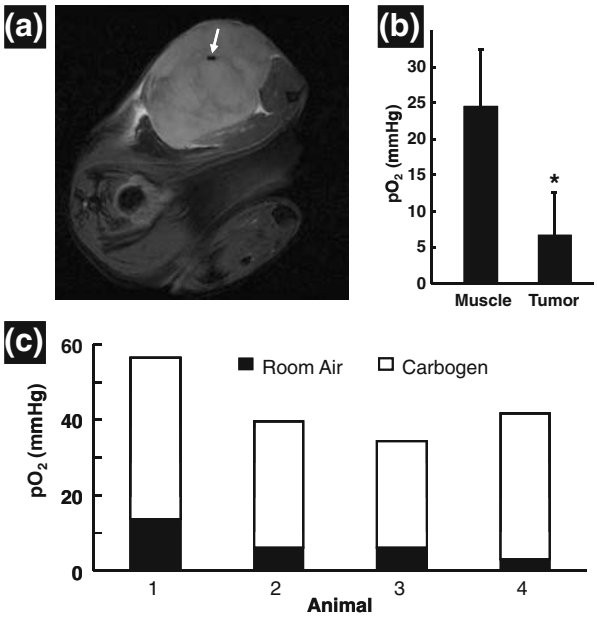

Fig. 6 *In vivo* functional testing of the LiNc-BuO:PDMS chip. The functional performance of the LiNc-BuO:PDMS chip was tested in a murine tumor model, which was developed by implanting RIF-1 tumor cells in the hind leg of the mice. (**a**) Representative MR image of a RIF-1 tumor implanted with a LiNc-BuO:PDMS chip, acquired on an 11.7 T MRI system. White arrow in the image indicates the location of the implanted LiNc-BuO:PDMS chip within the tumor mass. (**b**) Tumor pO_2 measurement using the LiNc-BuO:PDMS chip. L-band EPR spectroscopy was used to monitor the pO_2 reported by the LiNc-BuO:PDMS chip implanted in the tumor, as well as, the gastrocnemius muscle tissue on the contralateral side (control). Data are represented as mean ± SD (n=4). Measurements were made on the second day after surgical implantation of the chips in the tumor and muscle. It can be observed that the implanted chips were capable of sensing the hypoxia in the tumors, with a significant difference ($p< 0.05$) compared to muscle (control). (**c**) Response of the LiNc-BuO:PDMS chip to changes in tumor pO_2. The ability of the implanted chip to detect changes in tumor pO_2 was tested by switching the breathing gas (delivering the isoflurane anesthesia to the mice) from room air to carbogen (95% O_2, 5% CO_2). The implanted chips reported a consistent increase in tumor pO_2 upon carbogen-breathing. Overall, the results establish the suitability of the LiNc-BuO:PDMS chip for clinically relevant *in vivo* applications

muscle (control). The average RIF-1 tumor pO_2 reported by the implanted chip was 6.7±5.8 mmHg, which is in agreement with previously reported pO_2 values for this particular tumor type (Bratasz et al. 2007; Ilangovan et al. 2004a). Mice were then subjected to carbogen-breathing, in order to test the ability of the implanted chip to respond to changes in tumor pO_2. Carbogen-breathing caused an increase in the oxygenation of tumors. Fig. 6(c) shows that the implanted chip reported an increase in measured tumor pO_2, as is expected with carbogen-breathing. Disparities in baseline tumor pO_2 (pO_2 under room air-breathing) between animals can be attributed to relative differences in the level of hypoxia in the tumors themselves, and the location of the chips within these tumors. When the

breathing gas was switched back to room air from carbogen, the tumor pO_2 returned back to baseline levels (data not shown). Overall, these results confirmed the applicability of the LiNc-BuO:PDMS chip for tumor oximetry.

4 Conclusions

We have demonstrated preliminary biological evaluation and functional testing of biocompatible EPR oximetry sensors, the LiNc-BuO:PDMS chips, made by the encapsulation of microcrystals of LiNc-BuO in PDMS. The chips were not affected by sterilization procedures or high-energy radiation. They exhibited excellent *in vitro* biostability and biocompatibility, as was established by exposing them to oxidoreductants and co-incubating them with cells. The suitability and applicability of these novel oxygen sensors for long-term *in vivo* oximetry was demonstrated by monitoring the oxygenation of murine muscle tissue for an extended period. The sensors were also found to exhibit good *in vivo* biocompatibility, with no adverse effect on oxygen-sensing ability due to extended *in vivo* residence. Further, testing in a murine tumor model showed that the LiNc-BuO:PDMS chip can be used to obtain reliable measurements of tumor oxygenation. Overall, we have established the LiNc-BuO:PDMS chip as a promising choice of probe for clinical EPR oximetry.

Acknowledgments This study was supported by NIH grant EB004031. We would like to thank Dr. Charles Hitchcock for his assistance with histological analysis.

References

J.M. Anderson. Cardiovasc. Pathol. **4**, 33S–41S (1993) doi:10.1016/1054-8807(93)90045-4

A. Bratasz, R.P. Pandian, Y. Deng, S. Petryakov, J.C. Grecula, N. Gupta, P. Kuppusamy. Magn. Reson. Med. **57**(5), 950–959 (2007) doi:10.1002/mrm.21212

F. Denizot, R. Lang. J. Immunol. Methods **89**(2), 271–277 (1986) doi:10.1016/0022-1759(86)90368-6

A. Dinguizli, S. Jeumont, N. Beghein, J. He, T. Walczak, P.N. Lesniewski, H. Hou, O.Y. Grinberg, A. Sucheta, H.M. Swartz, B. Gallez. Biosens. Bioelectron. **21**(7), 1015–1022 (2006) doi:10.1016/j.bios.2005.03.009

M. Dinguizli, N. Beghein, B. Gallez. Physiol. Meas. **29**(11), 1247–1254 (2008) doi:10.1088/0967-3334/29/11/001

P.R. Dvornic, Thermal Properties of Polysiloxanes at Low Temperatures, in *Silicon-Containing Polymers - The Science and Technology of Their Synthesis and Applications*, ed. by R.G. Jones, W. Ando, J. Chojnowski (Kluwer Academic Publishers, Norwell, MA, 2000), pp. 185–212

E. Eteshola, R.P. Pandian, S.C. Lee, P. Kuppusamy. Biomed. Microdevices. **11**(2), 379–387 (2009)

B. Gallez, K. Mader. Free Radic. Biol. Med. **29**(11), 1078–1084 (2000) doi:10.1016/S0891-5849(00)00405-6

H.W. Hopf, M.D. Rollins. Antioxid. Redox Signal. **9**(8), 1183–1192 (2007) doi:10.1089/ars.2007.1641

G. Ilangovan, A. Bratasz, H. Li, P. Schmalbrock, J.L. Zweier, P. Kuppusamy. Magn. Reson. Med. **52**(3), 650–657 (2004a) doi:10.1002/mrm.20188

G. Ilangovan, H. Li, J.L. Zweier, P. Kuppusamy. J. Phys. Chem. B **105**, 5323–5330 (2001) doi:10.1021/jp010130+

G. Ilangovan, A. Manivannan, H.Q. Li, H. Yanagi, J.L. Zweier, P. Kuppusamy. Free Radic. Biol. Med. **32**(2), 139-147 (2002a) doi:10.1016/S0891-5849(01)00784-5

G. Ilangovan, R. Pal, J.L. Zweier, P. Kuppusamy, J. Phys. Chem. B **106**, 11929–11935 (2002b). doi:10.1021/jp026360l

G. Ilangovan, J.L. Zweier, P. Kuppusamy. J. Magn. Reson. **170**(1), 42–48 (2004b) doi:10.1016/j.jmr.2004.05.018

M. Khan, K.M. Iyyapu, V. Kutala, S. Kotha, N.L. Parinandi, R.L. Hamlin, P. Kuppusamy, Antioxid. Redox. Signal. (2008)

M. Khan, V.K. Kutala, D.S. Vikram, S. Wisel, S.M. Chacko, M.L. Kuppusamy, I.K. Mohan, J.L. Zweier, P. Kwiatkowski, P. Kuppusamy. Am. J. Physiol. Heart Circ. Physiol. **293**(4), H2129–H2139 (2007) doi:10.1152/ajpheart.00677.2007

N. Khan, B.B. Williams, H. Hou, H. Li, H.M. Swartz. Antioxid. Redox Signal. **9**(8), 1169–1182 (2007) doi:10.1089/ars.2007.1635

A.C. Kulkarni, P. Kuppusamy, N. Parinandi. Antioxid. Redox Signal. **9**(10), 1717–1730 (2007) doi:10.1089/ars.2007.1724

V.K. Kutala, M. Khan, M.G. Angelos, P. Kuppusamy. Antioxid. Redox Signal. **9**(8), 1193–1206 (2007) doi:10.1089/ars.2007.1636

R.S. Labow, E. Meek, J.P. Santerre. J. Cell. Physiol. **186**(1), 95–103 (2001) doi:10.1002/1097-4652(200101)186:1<95::AID-JCP1008>3.0.CO;2-0

K.J. Liu, P. Gast, M. Moussavi, S.W. Norby, N. Vahidi, T. Walczak, M. Wu, H.M. Swartz. Proc. Natl. Acad. Sci. USA **90**(12), 5438–5442 (1993) doi:10.1073/pnas.90.12.5438

S.P. Marso, W.R. Hiatt. J. Am. Coll. Cardiol. **47**(5), 921–929 (2006) doi:10.1016/j.jacc.2005.09.065

G. Meenakshisundaram, E. Eteshola, R.P. Pandian, A. Bratasz, S.C. Lee, P. Kuppusamy, Biomed. Microdevices. (Epub ahead of print) (2009)

I.K. Mohan, M. Khan, S. Wisel, K. Selvendiran, A. Sridhar, C.A. Carnes, B. Bognar, T. Kalai, K. Hideg, P. Kuppusamy, Am. J. Physiol. Heart. Circ. Physiol. **296**(1), H140–151 (2009)

R.P. Pandian, Y.I. Kim, P.M. Woodward, J.L. Zweier, P.T. Manoharan, P. Kuppusamy, J. Mater. Chem. **16**(36), 3609–3618 (2006)

R.P. Pandian, N.L. Parinandi, G. Ilangovan, J.L. Zweier, P. Kuppusamy, Free Radic. Biol. Med. **35**(9), 1138–1148 (2003)

R. Springett, H.M. Swartz, Antioxid. Redox. Signal. **9**(8), 1295–1301 (2007)

H.M. Swartz, Antioxid. Redox. Signal. **6**(3), 677–686 (2004)

P. Vaupel, M. Hockel, A. Mayer, Antioxid. Redox. Signal. **9**(8), 1221–1235 (2007)

D.S. Vikram, J.L. Zweier, P. Kuppusamy, Antioxid. Redox. Signal. **9**(10), 1745–1756 (2007)

S. Wisel, S.M. Chacko, M.L. Kuppusamy, R.P. Pandian, M. Khan, V.K. Kutala, R.W. Burry, B. Sun, P. Kwiatkowski, P. Kuppusamy, Am. J. Physiol. Heart. Circ. Physiol. **292**(3), H1254–H1261 (2007)

J.L. Zweier, A. Samouilov, M. Chzhan. J Magn Reson B **109**(3), 259–263 (1995)